

In situ electrical conductivity measurements of porous water-containing rock materials under high temperature and high pressure conditions in an autoclave

Cite as: Rev. Sci. Instrum. **92**, 095104 (2021); <https://doi.org/10.1063/5.0054892>

Submitted: 22 April 2021 • Accepted: 27 August 2021 • Published Online: 21 September 2021

 Shuangming Shan,  Chaoyi Xiao,  Heping Li, et al.



View Online



Export Citation



CrossMark

ARTICLES YOU MAY BE INTERESTED IN

[Rotational speed sensor based on the magnetoelectric effect of composite FeSiB/Pb\(Zr,Ti\)O₃](#)

Review of Scientific Instruments **92**, 095009 (2021); <https://doi.org/10.1063/5.0062662>

[Fabrication of spectroscopic characterization techniques using an optical fiber-based spectrometer](#)

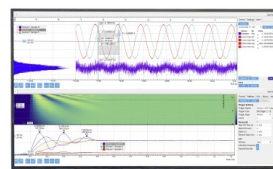
Review of Scientific Instruments **92**, 093104 (2021); <https://doi.org/10.1063/5.0054308>

[Development of a flexure-based nano-actuator for high-frequency high-resolution directional sensing with atomic force microscopy](#)

Review of Scientific Instruments **92**, 093703 (2021); <https://doi.org/10.1063/5.0057032>

Challenge us.

What are your needs for periodic signal detection?



Zurich Instruments

In situ electrical conductivity measurements of porous water-containing rock materials under high temperature and high pressure conditions in an autoclave

Cite as: Rev. Sci. Instrum. 92, 095104 (2021); doi: 10.1063/5.0054892

Submitted: 22 April 2021 • Accepted: 27 August 2021 •

Published Online: 21 September 2021



View Online



Export Citation



CrossMark

Shuangming Shan,¹ Chaoyi Xiao,^{1,2} Heping Li,^{1,a)} Liping Xu,^{1,3} Sen Lin,¹ and Shengbin Li¹

AFFILIATIONS

¹ Key Laboratory for High-Temperature and High-Pressure Study of the Earth's Interior, Institute of Geochemistry, Chinese Academy of Sciences, Guiyang, Guizhou 550081, China

² University of Chinese Academy of Sciences, Beijing 100049, China

³ Zhejiang Pharmaceutical College, Ningbo 315100, China

^{a)} Author to whom correspondence should be addressed: liheping@mail.gyig.ac.cn

ABSTRACT

This study presents a method for measuring the electrical conductivity of porous rock materials *in situ* under a shallow Earth crust environment simulated according to temperature, confining pressure, and liquid water saturation in a high-temperature autoclave. The sample was first encased within a poly tetra fluoroethylene container with two Pt wires leading out and was then placed into the high-temperature autoclave. The lead wires were connected to an external measurement system after passing through the autoclave sealing plug. The electrical conductivity of sandstone was measured under different temperatures (30, 60, 90, 120, 150 °C), liquid water saturation levels (36%, 51%, 100%), and 2 MPa by using this method. The electrical conductivity of the sandstone samples increased with increasing temperature and also increased as the level of water saturation increased. All the results agreed well with the Arrhenius relationship, Archie's law, and previous experimental study. This method can be used to measure other kinds of porous water-containing rocks, and the results can be applied in geothermal/oil research.

Published under an exclusive license by AIP Publishing. <https://doi.org/10.1063/5.0054892>

I. INTRODUCTION

Measuring electrical conductivity of rocks is of critical importance for oil and mineral exploration.¹ Geoelectrical measurements are a useful, nondestructive tool for characterizing porous rocks and soils.² Its main interest lies in its sensitivity to key properties of storage and transport in porous media.³

The characterization of rock materials embedded within the Earth is essential for supporting engineering activities, such as exerting the productivity of sandstone reservoir and enhancing the recovery efficiency of oil/gas.⁴ In addition, the characterization of the electrical conductivity of underground rock materials is of great interest. For example, it can be used to study the pore structure character of reservoir rapidly and efficiently by introducing the electrical conductivity data and provide a guarantee for the exploration and exploitation.⁵ On the other hand, it is a good survey method for

geothermal exploration, which cannot only explore the depth and the fragmentation of the stratum but also predict the hydrous property of the structures that contain thermal.⁶

However, the required measurements often cannot be performed at all for rock materials *in situ* or cannot be conducted without drastically disturbing the environment, and thereby detracting from the accuracy of results. Therefore, numerous efforts have been made to develop methods for electrical conductivity measurement at high temperature and high pressure conditions. The most common high temperature and high pressure equipment currently employed for this purpose include autoclaves, Paterson press apparatus,^{7,8} piston cylinder apparatus,^{9–12} multi-anvil apparatus,^{13–19} and diamond anvil cell.^{20–22} However, few efforts have been made in autoclave, which is suitable for simulating the shallow Earth crust environment.

Morey²³ first used autoclaves in preparing silicates over 100 years ago. Plenty of researchers used autoclaves as the main

apparatus in their study.^{24–27} Autoclaves generally employ water as the pressure transmitting medium. This is not suitable when the electrical conductivity of the sample is to be determined unless steps are taken to ensure that the sample system is electrically insulated. In addition, special treatment is required to isolate the metal autoclave body from the conductive wires employed in the measurement process. Moreover, liquid water is generally present in shallow Earth crust environments, and special methods must be adopted when simulating different levels of liquid water saturation. The most common method is to seal the water-containing sample within a ductile and chemically stable metal enclosure.^{28–32} The sealing employed must be particularly secure to both maintain the pressure of the autoclave system³³ and to prevent water vaporization and escape under the high temperature conditions. However, the use of a metal sealing system is again unsuitable when the electrical conductivity of the sample is to be determined, particularly for low conductivity geological samples.

According to the above discussion, electrical insulation and mechanical sealing of the autoclave and sample are the two key issues that must be confronted when measuring the conductivity of rock samples in a simulated shallow Earth crust environment under high temperature and confining pressure conditions with varying degrees of liquid water saturation.

This study introduces a method for solving these two key issues. Rock samples are first encased within a sample sealing device to ensure sample isolation and electrical insulation, and lead wires are connected at both ends of the device to enable electrical conductivity measurements. The sealed sample is then placed in the high-temperature autoclave (high-purity argon works as the pressure

transmitting medium), and the lead wires connected to an external measurement system after passing through the autoclave sealing plug. The functionality of the proposed method is demonstrated by its application for measuring the electrical conductivity of sandstone samples under different temperatures, confining pressures, and liquid water saturations.

II. EXPERIMENTAL

A. Mechanical sealing and electrical insulation of the autoclave

After considerable efforts to obtain a material that provided sufficient mechanical toughness and very low electrical conductivity, alumina ceramic was found to be a suitable sealing material that could successfully seal the autoclave for pressure less than 350 MPa, and its electrical insulation performance could meet the experimental requirements.

As shown in Fig. 1, two platinum wires (0.3 mm in diameter) were sintered separately in the center of an alumina ceramic cone. The alumina ceramic cone was designed and tested by us and manufactured by Tangshan Advanceram Ltd., China. Then, the alumina ceramic cone was pressed into the autoclave sealing plug with a red copper cone sleeve. The high pressure acting between the red copper cone sleeve, the alumina ceramic cone, and the sealing plug prevented the escape of the internal pressure of the autoclave. Moreover, because the internal pressure of the autoclave was greater than the external pressure, the contacts between the alumina ceramic cone, the alumina ceramic cone sleeve, and the sealing plug were self-tightening.

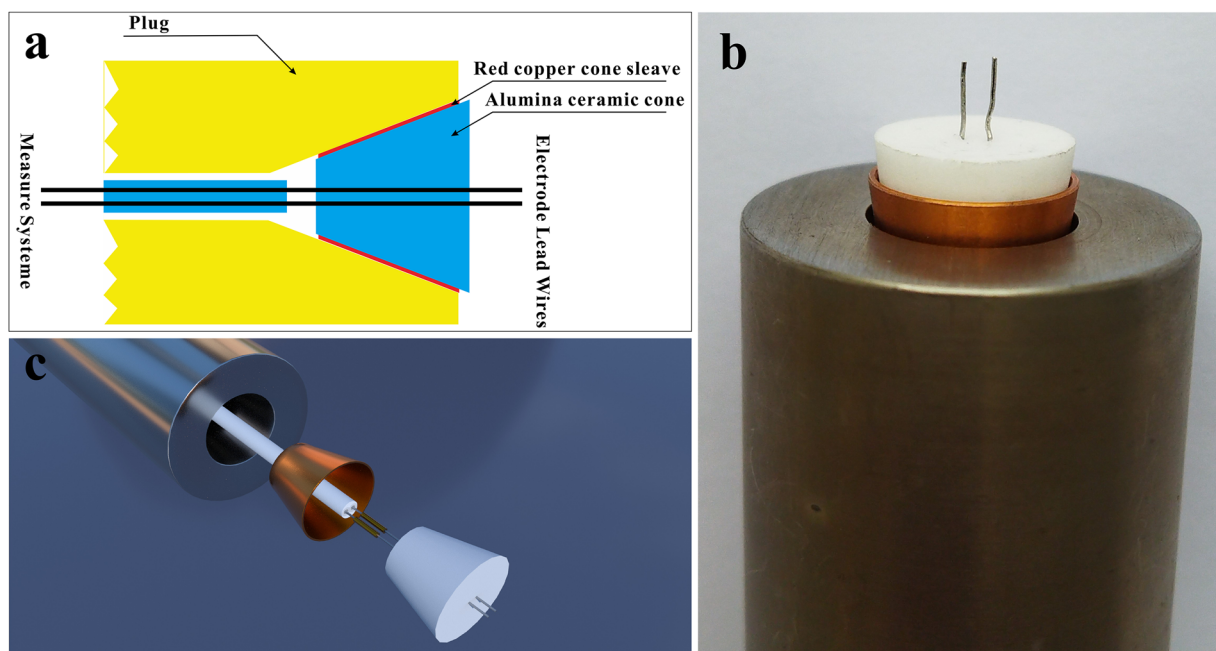


FIG. 1. Schematic diagram of the alumina ceramic cone, the alumina ceramic cone sleeve, and the sealing plug system. (a) is the axial section image; (b) is the real picture, which shows the situation before pressing the alumina cone into the plug; and (c) is the 3D image.

In addition, the autoclave was externally heated in a resistance furnace, and the pressure in the autoclave was adjusted using a gas pressurizing device connected to the end of the autoclave. The maximum pressure the gas pressurizing device can generate is 400 MPa.³⁴

The proposed autoclave sealing design was tested as follows. After sealing the autoclave, the autoclave was heated to 150 °C and maintained at that temperature, and then, the autoclave was pressurized to 350 MPa with high-purity argon gas. The autoclave was supplied with no additional argon gas input during subsequent testing (the gas pressurizing device can adjust and keep pressure automatically, but it was disabled here for testing). Then, the autoclave had maintained at that temperature and pressure for 24 h. The internal pressure of the autoclave was monitored and found to be kept at 350 MPa all the time. The results demonstrated that the autoclave was effectively sealed by this method.

B. Mechanical sealing and electrical insulation of the sample

A two-sleeved cylindrical sample container was fabricated from poly tetra fluoroethylene (PTFE) for housing cylindrical rock samples, as illustrated in Fig. 2.

The cylindrical rock samples were obtained by using a drill machine with a standard diameter of 10.0 mm and length of 14.0 mm. The inner and outer PTFE sleeves were combined by means of a reverse buckle configuration such that the action of the external pressure on the sample container could ensure good sealing. The internal dimensions of the inner sleeve were designed to precisely match the outer dimensions of the rock sample, and both sleeves were fabricated with uniform wall thicknesses of 1.0 mm. Pan *et al.*¹⁹ also used PTFE as the sample capsule when they measured electrical conductivity in multi-anvil apparatus because PTFE maintains high strength and toughness, making it a good sealing material for liquid samples.

Each electrode lead wire was threaded through its respective sleeve via a 0.3 mm diameter hole drilled in the bottom of each PTFE

sleeve. The two sleeves and the wires were further sealed by applying high temperature (less than 200 °C) AB glue (Shenzhen Blue Road New MSTAR Technology Ltd., China). The silver electrodes were applied using Ag electrical conductive adhesive (Sino-Platinum Metals Ltd., China). The resulting electrodes were ~0.15 mm thick. Eitner *et al.*³⁵ measured the contact resistance of three kinds of adhesives by the transmission line method (TLM) and found that the maximum contact resistance of a 2 × 2 mm² adhesive was 1.3 Ω. Xiao and He³⁶ measured the contact resistance of Ag-conductive adhesives up to 210 °C and found that the maximum contact resistance is about 250 mΩ. In this study, the minimum resistance of the sample is about 1 kΩ, which is about 3 orders of magnitude higher than the contact resistance, so the contact resistance of the Ag-adhesive electrode could be ignored. The lead wires were crimped to ensure good electrical connectivity to the silver electrodes due to their high conductivity and malleability.

The proposed sample sealing design was tested as follows:

- (i) A dry cylindrical porous sandstone sample with applied silver electrodes was weighed, and the sample mass was recorded as m_1 . The sample was then immersed in filtered water for 48 h, and the sample mass was again measured and recorded as m_2 .
- (ii) After encasing the sample as shown in Fig. 2, it was placed in the autoclave at room temperature, and the autoclave was filled with high-purity argon gas to an internal pressure of 2 MPa. The signal from the electrode lead wires was not monitored.
- (iii) The autoclave was heated to 150 °C and maintained at that temperature for 24 h and then was cooled down to room temperature.
- (iv) The sample was removed from the autoclave after releasing pressure, unpacked from the sample container, and weighed. The mass of the sample was recorded as m_3 , and a comparison indicated that $m_2 \approx m_3$, demonstrating that the sample was effectively sealed in the autoclave by this method.

C. Electrical conductivity measurement

The specific method for measuring the electrical conductivity of rock samples using the proposed system is illustrated in Fig. 3 and can be described as follows:

- (i) Silver electrodes were applied to cylindrical rock samples of the appropriate dimensions, and the sample was immersed in the liquid for an appropriate duration, depending on the desired state of saturation.
- (ii) The sample was sealed and installed within the autoclave as shown in Fig. 3, and the lead wires were connected to the electrical conductivity measurement system (Solartron 1296 Dielectric Interface and Solartron 1260 Impedance/Gain-phase Analyzer).
- (iii) The autoclave was externally heated to the desired temperature.
- (iv) High-purity argon was injected into the autoclave until obtaining the desired pressure.
- (v) The electrical conductivity of the sample was then monitored *in situ* at different temperatures, confining pressures, and liquid saturations.

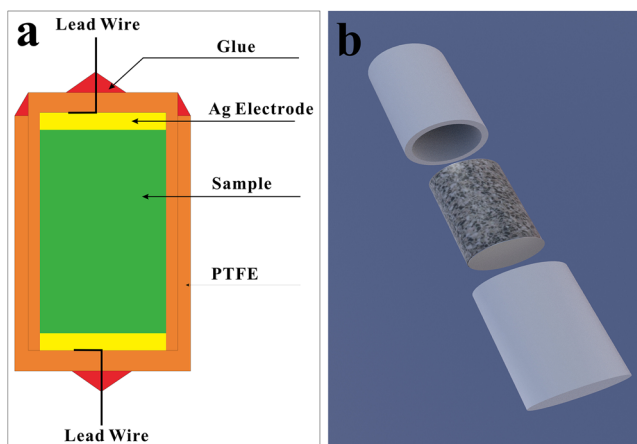


FIG. 2. Schematic diagram of the PTFE sample sealing sleeves and sample. (a) is the axial section image; (b) is the 3D image.

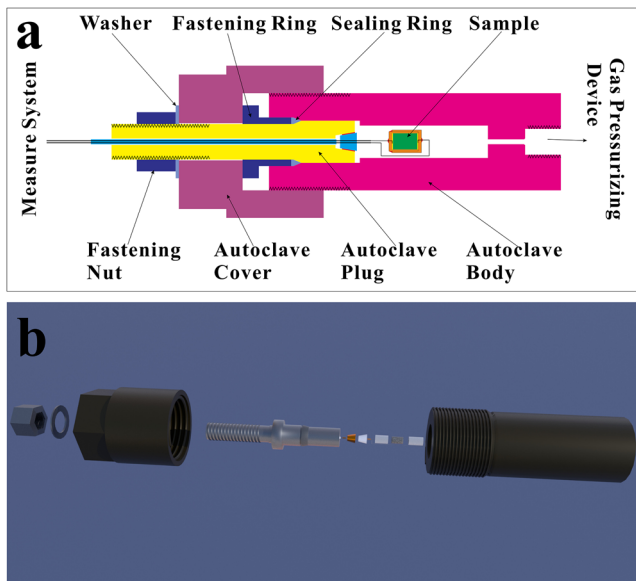


FIG. 3. Assembly diagram for conducting electrical conductivity measurements *in situ* (all the exposed wires were protected in an alumina tube for electrical insulation). (a) is the axial section image; (b) is the 3D image.

III. RESULTS

Before measuring rock samples, we measured the resistance of a PTFE disk with 3 mm in thickness and 10 mm in diameter at a pressure of 2 MPa and temperatures of 30, 60, 90, 120, and 150 °C *in situ*. We found that the resistances were 0.2, 0.7, 1.3, 2.6, and 4.7 T Ω , respectively. These values were around the upper detection limit of Solartron 1260 and Solartron 1296. The resistance increased with increasing temperature slightly, and it might be because the absorbed water of the insulation system (alumina cone, alumina tube, and PTFE sleeves) escaped when heating. The most important was that the values were 5–6 orders of magnitude higher than the resistance of the sandstone samples with different levels of liquid saturation, which was about 1.0 M Ω maximum. This meant that the insulation system was good enough for our measurements.

The proposed system was applied to measure the electrical conductivity σ_b of bulk sandstone samples with different levels of liquid saturation at a pressure of 2 MPa and temperature values of 30, 60, 90, 120, and 150 °C *in situ*. The sandstone samples were obtained from Henan Province, China. Figure 4 showed the SEM images of the sample. The sample contained quartz (~50%), feldspar (~20%), and calcite as matrix (~30%). The average porosity of the samples was 15.2%. The liquid employed was NaCl water solution, the concentration was 0.2 ppm, and the electrical conductivity at room temperature was 3.85 S/m.

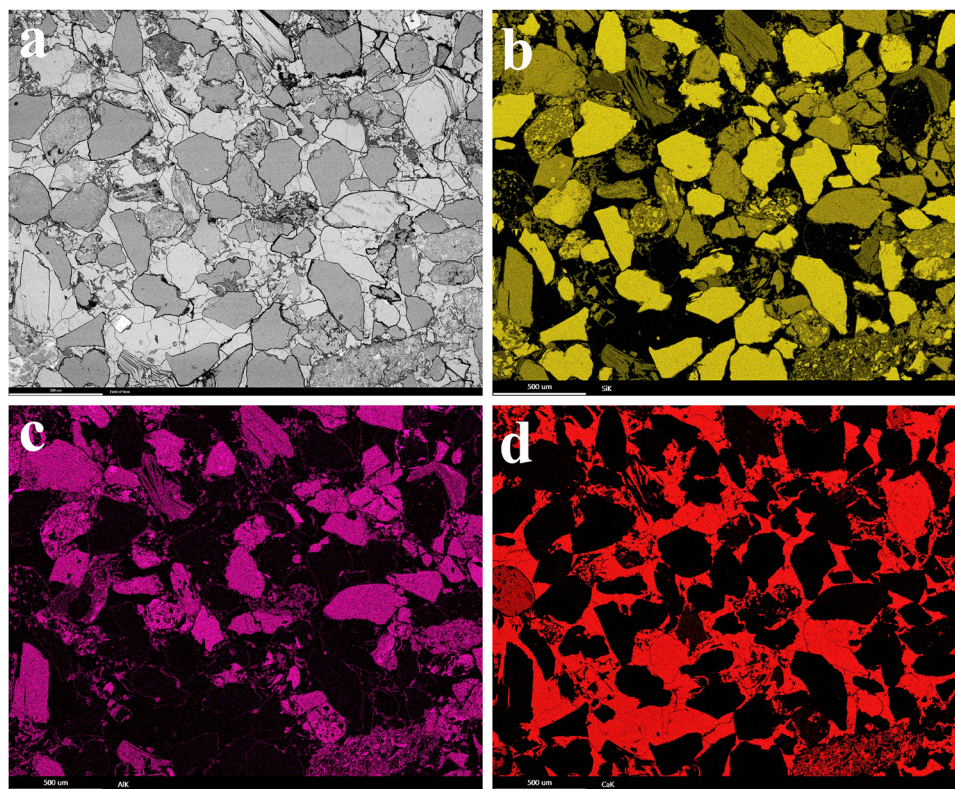


FIG. 4. SEM images of the sample. (a) is BSE image, and (b)–(d) are EDS mapping images of Si (yellow), Al (purple), and Ca (red), respectively.

The results of $\log \sigma_b$ obtained for the sandstone samples were plotted with respect to $10000/T$ in Fig. 5. We found that the $\log \sigma_b$ values exhibited a good linear relationship with $1/T$, indicating that σ_b obeyed the following Arrhenius relationship:

$$\log \sigma_b = \log \sigma_0 + \log \exp(-E/kT), \quad (1)$$

where $\log \sigma_0$ is a pre-exponential factor, k is the Boltzmann constant, E is the activation enthalpy, and T is absolute temperature. The parameters of the above Arrhenius relationship obtained from fitting for each sample were listed in Table I along with the coefficient of determination values R^2 reflecting the goodness of fit.

In addition, we plotted the values of $\log \sigma_b$ as a function of $\log \phi$ in Fig. 6 for the values of T considered. It can be seen that the results present an approximately linear relationship according to Archie's law,³⁷

$$\sigma_b = C\phi^n \sigma_f \quad \text{or} \quad \log \sigma_b = n \log \phi + b, \quad (2)$$

where n and C are constants and $b = \log C \log \sigma_f$. The parameters obtained by fitting the experimental data to Eq. (2) are listed in Table II.

It can be seen from the reported results that, as expected, the values of σ_b increased with increasing T and that the values of σ_b also increased as the level of water saturation increased. Moreover, the experimental results well satisfied both the Arrhenius relationship and Archie's law.

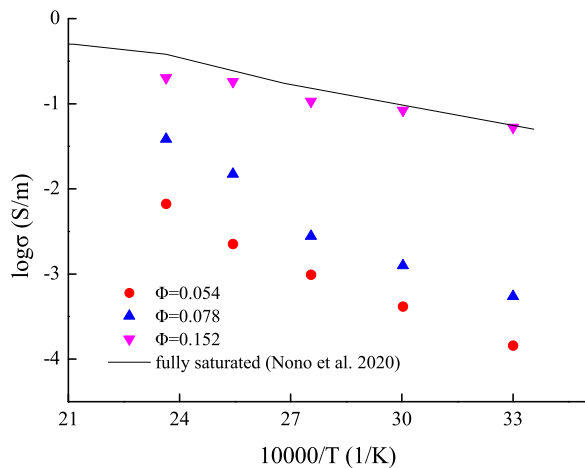


FIG. 5. Base 10 logarithm of the product of the electrical conductivity and temperature with respect to $1/T$ obtained for sandstone samples with different levels of saturation at a pressure of 2 MPa.

TABLE I. Parameters obtained from fitting the data in Fig. 5 according to the Arrhenius relationship in Eq. (1) for samples with different liquid saturation levels at a pressure of 2 MPa.

Sample	Saturation (%)	Volume fraction	$\log \sigma_0$	E (eV)	R^2
A	36	0.054	1.81	0.34	0.9883
B	51	0.078	3.22	0.40	0.9545
C	100	0.152	0.84	0.13	0.9774

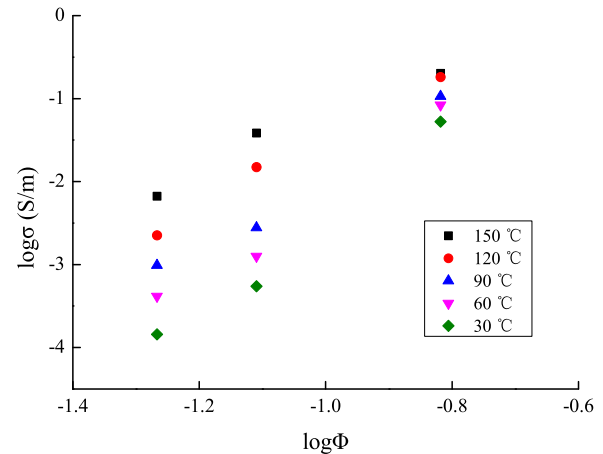


FIG. 6. Base 10 logarithm of σ_b with respect to the logarithm of the volume fraction of solution obtained for sandstone samples at different values of T and a pressure of 2 MPa.

TABLE II. Parameters obtained from fitting the data in Fig. 6 according to Archie's law in Eq. (2) for samples with different saturation levels at a pressure of 2 MPa.

Temperature ($^{\circ}$ C)	n	b	R^2
30	5.8496	3.4356	0.9818
60	5.2779	3.1662	0.9767
90	4.6488	2.7717	0.9185
120	4.1856	2.7191	0.9916
150	3.1932	1.9711	0.9651

Nono *et al.*⁸ measured the electrical conductivity of hydrothermally altered rocks at a confining pressure of 100 MPa, a pore fluid pressure up to 30 MPa, and temperatures up to 700 $^{\circ}$ C in Paterson press. In their work, the fluid was also the NaCl water solution, the electrical conductivity at room temperature was 3.9 S/m, and the porosity was 13.4(2.8)%. Figure 5 also shows a comparison between Nono's data and the present experimental data in the form of Arrhenius plot. Our fully saturated data show high quality of agreements with their data, which demonstrates that the proposed measurement system that provided electrical conductivity measurements of sandstone samples under different temperatures and liquid saturation levels at a given confining pressure is reliable.

This method can also be used to measure the other kinds of porous rocks, and the results may be applied in geothermal/oil research.

IV. CONCLUSIONS

This paper presented a method for measuring the electrical conductivity of porous rock materials *in situ* under a shallow Earth crust environment simulated according to temperature, confining pressure, and liquid water saturation in a high-temperature autoclave.

The proposed method was first verified to address the critical issue of the reliable sealing of the high-temperature and high-pressure autoclave to maintain a uniform pressure and of the sample

to maintain the initial water saturation level as well as the critical issue of ensuring the appropriate electrical insulation required for conducting accurate electrical conductivity measurements in close contact with metal components. The functionality of the proposed method was demonstrated by its application for measuring the electrical conductivity of sandstone samples under different temperature and liquid saturation levels at a confining pressure of 2 MPa. The results indicated that, as expected, the electrical conductivity of the sandstone samples increased with increasing temperature, and the electrical conductivity also increased as the level of water saturation increased. Finally, the experimental results agreed well with the Arrhenius relationship, Archie's law, and previous experimental study.

Accordingly, we conclude that the proposed measurement system provided electrical conductivity measurements that responded appropriately to the temperature and water saturation states of the sandstone samples. This method can be used to measure the other kinds of porous rocks, and the results can be applied in geothermal/oil research.

ACKNOWLEDGMENTS

The authors acknowledge LetPub for their language service. This research was financially supported by the Major State Research Development Program of China (Grant No. 2016YFC0601101) and the National Natural Science Foundation of China (Grant No. 41472048).

DATA AVAILABILITY

The data that support the findings of this study are available from the corresponding author upon reasonable request.

REFERENCES

- ¹J. G. Speight, *An Introduction to Petroleum Technology, Economics, and Politics* (Scrivener Publishing LLC, 2011).
- ²P. W. J. Glover, *Treatise on Geophysics*, 2nd ed. (Elsevier, 2015), Vol. 11, p. 89.
- ³D. T. Luong, J. Damien, V. D. Phan, and V. Nguyen, *Geophys. J. Int.* **219**(2), 866 (2019).
- ⁴J. Ouyang, *Oil Logging Interpretation and Reservoir Description* (Petroleum Industry Press, Beijing, 1994).
- ⁵J. Chen, X. Liu, Z. Cheng, X. Yang, H. Liu, and G. Zhou, *J. Southwest Pet. Inst.* **27**, 5 (2005).
- ⁶Y. Meng, Z. Zhang, and R. Liu, *Comput. Tech. Geophys. Geochem. Explor.* **32**, 31 (2010).
- ⁷M. Violay, B. Gibert, P. Azais, P. A. Pezard, and G. Lods, *Transp. Porous Media* **91**, 303 (2012).
- ⁸F. Nono, B. Gibert, F. Parat, D. Loggia, S. B. Cichy, and M. Violay, *J. Volcanol. Geotherm. Res.* **391**, 106364 (2020).
- ⁹X. Yang, H. Keppler, C. Mccammon, H. Ni, Q. Xia, and Q. Fan, *J. Geophys. Res.: Atmos.* **116**, B04208, <https://doi.org/10.1029/2010JB008010> (2011).
- ¹⁰H. Ni, H. Keppler, M. A. G. M. Manthilake, and T. Katsura, *Contrib. Mineral. Petrol.* **162**, 501 (2011).
- ¹¹H. C. Watson and J. J. Roberts, "Assembly for electrical conductivity measurements in the piston cylinder device," U.S. patent 8193823 B2 (Jun. 5, 2012).
- ¹²X. Guo, B. Li, H. Ni, and Z. Mao, *J. Geophys. Res.: Solid Earth* **122**, 1777, <https://doi.org/10.1002/2016JB013524> (2017).
- ¹³Y. Xu and T. Shankland, *Science* **280**, 1415 (1998).
- ¹⁴T. Katsura, K. Sato, and E. Ito, *Nature* **395**, 493 (1998).
- ¹⁵D. Wang, M. Mookherjee, Y. Xu, and S. I. Karato, *Nature* **443**, 977 (2006).
- ¹⁶T. Yoshino, T. Matsuzaki, S. Yamashita, and T. Katsura, *Nature* **443**, 973 (2006).
- ¹⁷T. Yoshino, E. Ito, T. Katsura, D. Yamazaki, S. Shan, X. Guo, M. Nishi, Y. Higo, and K. I. Funakoshi, *J. Geophys. Res.: Solid Earth* **116**, B04202, <https://doi.org/10.1029/2010JB007801> (2011).
- ¹⁸A. Pommier and K. D. Leinenweber, *Am. Mineral.* **103**, 1298 (2018).
- ¹⁹Y. Pan, W. Yong, and R. A. Secco, *Geophys. Res. Lett.* **47**, e2020GL090192, <https://doi.org/10.1029/2020GL090192> (2020).
- ²⁰H. Ni and Q. Chen, *Rev. Sci. Instrum.* **85**, 115107 (2014).
- ²¹L. Dai, L. Wu, H. Li, H. Hu, Y. Zhuang, and K. Liu, *J. Phys.: Condens. Matter* **28**, 475501 (2016).
- ²²L. Dai, C. Pu, H. Li, H. Hu, K. Liu, L. Yang, and M. Hong, *Rev. Sci. Instrum.* **90**, 066103 (2019).
- ²³G. W. Morey, *J. Am. Chem. Soc.* **36**, 514 (1914).
- ²⁴D. Gooch, *Ind. Eng. Chem.* **35**, 1304 (1943).
- ²⁵J. Wenzel and G. M. Schneider, *Rev. Sci. Instrum.* **52**, 1889 (1981).
- ²⁶G. Purser, C. A. Rochelle, H. C. Wallis, J. Rosenqvist, A. D. Kilpatrick, and B. Yardley, *Rev. Sci. Instrum.* **85**, 086109 (2014).
- ²⁷S. Klemme, M. Feldhaus, V. Potapkin, M. Wilke, M. Borchert, M. Louvel, A. Loges, A. Rohrbach, P. Weitkamp, E. Welter, M. Kokh, C. Schmidt, and D. Testemale, *Rev. Sci. Instrum.* **92**, 063903 (2021).
- ²⁸J. Arndt and N. Rombach, *J. Cryst. Growth* **35**, 28 (1976).
- ²⁹K. H. Becker, L. Cemič, and K. E. O. E. Langer, *Geochim. Cosmochim. Acta* **47**, 1573 (1983).
- ³⁰A. C. Hack and J. A. Mavrogenes, *Am. Mineral.* **91**, 203 (2006).
- ³¹E. Ito, *Treatise on Geophysics* (Elsevier, 2007), p. 197.
- ³²J. Du, H. Li, H. Liu, and H. Chang, *Am. Mineral.* **105**, 1254 (2020).
- ³³S. Lin, H. Li, L. Xu, Y. Zhang, and C. Cui, *RSC Adv.* **7**, 033914 (2017).
- ³⁴S. Li, H. Li, S. Shan, L. Liu, and S. Lin, "Rapid loading device for 400 MPa ultrahigh-pressure gas," CN 201920270834.2 (2019).
- ³⁵U. Eitner, T. Geipel, S.-N. Holtzschke, and M. Tränitz, *Energy Procedia* **27**, 676 (2012).
- ³⁶L. Xiao and F. He, *Microelectronics* **46**, 576 (2016).
- ³⁷G. E. Archie, *Trans. Am. Inst. Min., Metall. Pet. Eng.* **146**, 54 (1942).